

# Electrochemical Impedance Spectroscopy Effects of Vanadium doped - Cobalt Ferrite Nanomaterials for Supercapacitor Applications

G. Gowrisankar <sup>a, b\*</sup>, R. Mariappan <sup>b</sup>, Emmanuvel Feon Ramesh <sup>a</sup>,  
M. Abishek <sup>a</sup>, M. Prithisha <sup>a</sup>

<sup>a</sup> Department of Physics, Sri Ramakrishna College of Arts & Science, Coimbatore-641006, India

<sup>b</sup> Department Physics, R&D Center, Adhiyamaan College of Engineering (Autonomous), Hosur-635109, India

\* Corresponding author Email: [gsankar21@gmail.com](mailto:gsankar21@gmail.com)

DOI: <https://doi.org/10.54392/ara2413>

Received: 04-05-2024; Revised: 09-07-2024; Accepted: 17-07-2024; Published: 30-07-2024

**Abstract:** Vanadium-assisted cobalt ferrite nanoparticles generated using the co-precipitation process have better structural, morphological, and electrochemical properties than pure cobalt ferrite. The remarkable crystallinity of the cubic crystal structure was confirmed by X-ray diffraction (XRD) investigation. The use of field emission scanning electron microscopy (FESEM) demonstrated the presence of vanadium and consistent elemental composition with cobalt ferrite, while energy dispersive X-ray analysis (EDAX) verified the spherical nanoparticles with an average size of around 20 nm. Electrochemical impedance spectroscopy (EIS) indicated significant improvements in electrochemical performance, with a reduction in equivalent series resistance (ESR) from 1.54  $\Omega$  to 1.22  $\Omega$  and charge transfer resistance from  $1.68 \times 10^{-3} \Omega$  to  $1.5 \times 10^{-3} \Omega$  for V-doped  $\text{CoFe}_2\text{O}_4$ . Additionally, lower internal and Warburg resistance values were observed for V-doped  $\text{CoFe}_2\text{O}_4$ , suggesting efficient ion transport and storage capabilities. These findings highlight the potential of vanadium-doped cobalt ferrite nanostructures as promising materials for next-generation supercapacitors, addressing critical challenges in energy storage for renewable energy systems and portable electronics. Future studies should concentrate on refining the synthesis procedure and investigating other dopants in order to significantly improve the efficiency of supercapacitors based on cobalt ferrite.

**Keywords:** Cobalt Ferrite, Supercapacitors, Internal resistance, EIS.

## 1. Introduction

Supercapacitors have emerged as attractive alternatives due to their high power density and quick charge-discharge times due to the worldwide energy crisis and the growing demand for effective energy storage solutions. The low specific capacitance and cycling stability of traditional materials are issues that have spurred new research aimed at improving the electrochemical performance of supercapacitors using novel materials. Promising materials for [1–3] supercapacitors include graphene, carbon nanotubes, manganese dioxide ( $\text{MnO}_2$ ), and nickel oxide (NiO). Graphene and carbon

nanotubes are known for their exceptional electrical conductivity, large surface area, and mechanical strength. These carbon-based materials are often used to create high-performance supercapacitor electrodes that exhibit excellent capacitive behavior and long cycle life. Manganese dioxide offers high theoretical capacitance and is abundant and environmentally friendly, making it a popular choice for supercapacitor research. Nickel oxide is also notable for its high capacitance and good electrochemical stability.

Transition metal oxides and ferrites have been extensively explored for their potential in

energy storage applications. Among them, cobalt ferrite ( $\text{CoFe}_2\text{O}_4$ ) has garnered significant attention due to its excellent electrical conductivity, chemical stability, and mechanical robustness. Current studies are advancing the field by synthesizing nanostructured cobalt ferrite materials, leveraging its cubic crystal structure and semiconducting properties, which are advantageous for electrochemical applications, facilitating efficient charge storage and discharge processes [4, 5]. Because of its strong magnetic characteristics, high electrical conductivity, and electrochemical stability, cobalt ferrite is being investigated for application in supercapacitors. Applications include energy storage systems for renewable energy sources, electric vehicles (EVs) for quick energy delivery, portable electronics for extended battery life, and grid stabilization by mitigating voltage and frequency fluctuations [6, 7]. Cobalt ferrite supercapacitors are also used in industrial applications to increase the performance and efficiency of heavy machinery, as well as in hybrid energy storage systems that combine the advantages of batteries and supercapacitors. They also serve in backup power supplies (UPS) to ensure smooth operation during power outages. While promising, challenges such as material synthesis, cost, and scalability remain for commercial viability [8].

Synthesis processes for cobalt ferrite typically involve several methods tailored to achieve nanostructured materials optimized for supercapacitor applications. These methods include sol-gel techniques, hydrothermal synthesis, co-precipitation, and thermal decomposition of precursors. Each approach offers control over particle size, morphology, and crystallinity, influencing the material's electrochemical performance [9, 10]. The magnetic properties of cobalt ferrite also contribute significantly to supercapacitor functionality. While primarily recognized for their electrical properties, cobalt ferrites' magnetic characteristics can influence their interaction with external magnetic fields, potentially enabling novel applications in energy harvesting or magnetic field-assisted charge/discharge processes. To further optimize cobalt ferrite's performance, researchers are investigating various dopants such as vanadium (V), chromium (Cr), and nickel (Ni), which modify the material's electronic band structure and enhance its

electrochemical activity.[10] [5, 8]Vanadium doping introduces defects into the cobalt ferrite lattice, promoting ion diffusion and improving charge transfer kinetics. Chromium doping can enhance electrical conductivity and electrochemical stability, while nickel doping improves overall capacitance and cycling stability. These synergistic enhancements significantly boost the overall performance of supercapacitors, effectively addressing critical challenges in energy storage technology [10, 11]. Future advancements in dopant-assisted cobalt ferrite hold substantial promise for developing next-generation supercapacitors capable of meeting the escalating demands of modern energy systems.

The combination of modern characterization techniques, including as X-ray diffraction (XRD), scanning electron microscopy (SEM), and electrochemical impedance spectroscopy (EIS), yields detailed insights into these materials' structural, morphological, and electrochemical properties. [12] In summary, cobalt ferrite's integration into supercapacitor electrodes represents a significant advancement due to its robust synthesis methodologies and the material's inherent electrical and magnetic properties. Future energy storage systems may benefit from supercapacitors if their performance is improved and their potential for use is increased through further study into the magnetic-electrochemical interaction of cobalt ferrite and its optimized nanostructure. [13, 14]

This work introduces an approach to enhancing the properties of cobalt ferrite nanoparticles through vanadium doping, achieved via the co-precipitation method. The notable enhancements in electrochemical performance, including decreased charge transfer resistance and comparable series resistance, emphasize the special advantages of vanadium inclusion. Additionally, the enhanced ion transport and storage capabilities, as evidenced by lower internal and Warburg resistances, underscore the potential of vanadium-doped cobalt ferrite nanostructures as superior materials for next-generation supercapacitors. This study offers new insights into the optimization of cobalt ferrite-based materials for advanced energy storage applications.

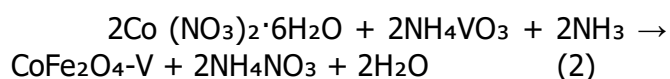
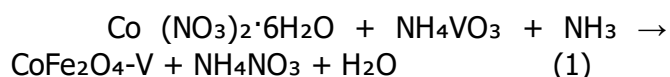
## 2. Experimental Details

### 2.1 Materials Used

Cobalt nitrate ( $\text{Co}(\text{NO}_3)_2$ ), Iron nitrate  $\text{Fe}(\text{NO}_3)_2$  ammonium metavanadate ( $\text{NH}_4\text{VO}_3$ ), ammonia ( $\text{NH}_3$ ), deionized water, ethanol, potassium hydroxide (KOH), N-methyl-2-pyrrolidinone ( $\text{C}_5\text{H}_9\text{NO}$ , NMP), and polyvinylidene fluoride ( $(-\text{C}_2\text{H}_2\text{F}_2)_n-$ , PVDF) were all procured from Sigma-Aldrich with analytical reagent (AR) grade and purity exceeding 98%, and were utilized without further modification.

### 2.2. Synthesis of Vanadium assisted Cobalt ferrite nanoparticles

To synthesize Cobalt ferrite ( $\text{CoFe}_2\text{O}_4$ ) and Vanadium assisted Cobalt ferrite ( $\text{CoFe}_2\text{O}_4\text{-V}$ ) nanoparticles ( $\text{CoFe}_2\text{O}_4\text{-V}$ ), we adopted a well-established coprecipitation method. Initially, the starting concentrations were set at 0.1 M for cobalt nitrate hexahydrate ( $\text{Co}(\text{NO}_3)_2 \cdot 6\text{H}_2\text{O}$ ) and 0.1 M for ammonium vanadate ( $\text{NH}_4\text{VO}_3$ ) in a 1:1 ratio [15, 16]. [17]. The reaction mixture's pH and particle size were carefully regulated by gradually adding little amounts (0.1 M) of ammonia ( $\text{NH}_3$ ), stirring constantly, and precisely adjusting the pH to 7. Equations (1) and (2) represent the chemical reactions occurring in the reaction mixture.



Centrifugation was used to collect the greenish-blue precipitate that, at reaction completion, indicated the synthesis of vanadium-assisted Cobalt ferrite nanoparticles, or  $\text{CoFe}_2\text{O}_4\text{-V}$ . After carefully decanting the supernatant to separate the precipitate, the precipitate was rinsed four times in a row with ethanol and water in alternate cycles to eliminate any remaining reactants. The resulting nanomaterials were then dried in an air oven for the entire night at  $80^\circ\text{C}$ , and then they were annealed for two hours at  $400^\circ\text{C}$ . This thermal treatment resulted in the formation of nanostructured  $\text{CoFe}_2\text{O}_4\text{-V}$ , enhancing its crystallinity and electrochemical properties. Importantly, this synthesis method demonstrates reproducibility under consistent reaction conditions.

### 2.3 Electrode preparation

Surface cleaning plays a crucial role in eliminating contaminants before electrode design. A composite comprising 80% by weight of synthetic Vanadium Assisted Cobalt Ferrite Nanoparticles ( $\text{CoFe}_2\text{O}_4\text{-V}$ ), 10% acetylene black, and 10% Polyvinylidene Fluoride (PVDF) was prepared in order to prepare the working electrode. To reach a surface area of  $1\text{ cm}^2$ , this composite was dissolved in N-methyl-2-pyrrolidinone (NMP) solvent to produce a slurry, which was subsequently sprayed onto a nickel foam substrate. After that, the coated substrate was dried for the entire night at  $80^\circ\text{C}$  in an air oven. [18]

The electrochemical performance of Vanadium assisted Cobalt ferrite nanoparticles ( $\text{CoFe}_2\text{O}_4\text{-V}$ ) electrode was assessed by means of a variety of electrochemical techniques, such as cyclic voltammetry (CV), galvanostatic charge-discharge (GCD), and electrochemical impedance spectroscopy (EIS). The electrochemical characterization provided significant insights into the behaviour and performance of the vanadium-assisted Cobalt ferrite nanoparticles ( $\text{CoFe}_2\text{O}_4\text{-V}$ ) electrode [19].

## 3. Result and Discussion

### 3.1 X-ray diffraction studies

Figure 1 displays the Cobalt Ferrite nanoparticles' XRD pattern. The  $2\theta$  values were fixed between  $20^\circ$  and  $70^\circ$ . The intensity values were taken from 1200 to 4800. The crystal system observed from the XRD technique is cubic. The empirical and chemical formula is  $\text{CoFe}_2\text{O}_4$ , and the second chemical formula is  $\text{CoO} \cdot \text{Fe}_2\text{O}_3$ . The space group were observed to be  $\text{Fd}3\text{m}$  and the space group number is 227 with cell parameters being  $a = b = c = 8.3919\text{ \AA}$ . Figure 1 displays the XRD spectra of the fresh and vanadium-doped  $\text{CoFe}_2\text{O}_4$  MNPs. The crystalline  $\text{CoFe}_2\text{O}_4$  (JCPDS 22-1086) showed seven distinct peaks at  $2\theta$  of  $30.1^\circ$ ,  $35.5^\circ$ ,  $43.1^\circ$ ,  $53.40^\circ$ ,  $56.9^\circ$ ,  $62.7^\circ$ , and  $73.9^\circ$ , which were indexed to the (2 2 0), (3 1 1), (4 0 0), (4 2 2), (5 1 1), (4 2 2), and (5 3 3) planes, respectively [20]. The calculated density from the XRD result is  $5.30\text{ g/cm}^3$ . The volume of a cell is given as  $590.99 \times 10^6\text{ pm}^3$ . The sample for XRD was made by heating co-precipitated hydroxides at  $950^\circ\text{C}$  for 40 hours.

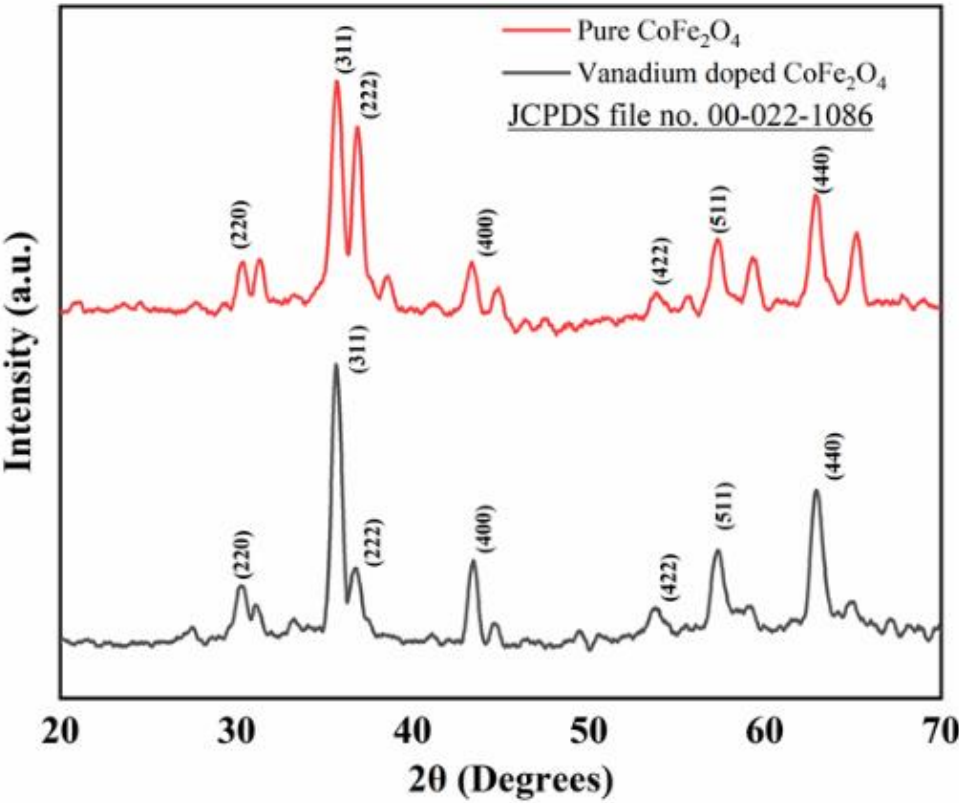


**Figure 1** XRD Pattern of Pure and Vanadium doped CoFe<sub>2</sub>O<sub>4</sub> nanoparticles.

**Table 1.** XRD Parameters of CoFe<sub>2</sub>O<sub>4</sub> & V doped CoFe<sub>2</sub>O<sub>4</sub>

Sample	β	Grain Size (D) (nm)	Interplanar Spacing (d) Å	Micro strain (t) (μm)	Dislocation Density m/m <sup>3</sup>
CoFe <sub>2</sub> O <sub>4</sub>	0.149	97	2.513	0.0355	0.01046
V+CoFe <sub>2</sub> O <sub>4</sub>	0.22	66	2.512	0.0523	0.02282

The XRD patterns were noted at 25° C. The highest peak from the XRD pattern of pure cobalt ferrite and vanadium doped cobalt ferrite is taken which is at 35.677° and 35.7° and both have h k l indices as (311). The peak is used to calculate the Full Width Half Maxima (β) value of the material, which can be used to find the grain size/crystal size (D) and Micro strain (t) of the material. From the peak of the Full Width Half Maxima, β = 0.149 and 0.22. Using the Scherrer formula which is given as

$$D = 0.9 \lambda / \beta \cos \theta \tag{3}$$

Using θ = 17.8385 and 17.85, the wavelength of the X-ray from the X-ray Diffractometer, λ = 1.54 Å and the β = 0.149 and 0.22 in the above formula the grain size, D = 97

nm and 66 nm [10]. The interplanar spacing (d) is found using the formula,

$$d = n \lambda / 2 \sin \theta \tag{4}$$

Where n = 1. The interplanar spacing, d = 2.5135 x 10<sup>-10</sup> m and 2.512 x 10<sup>-10</sup> m

The microstrain, which gives the degree of distortion present in the crystalline lattice is calculated using the formula,

$$t = \beta \cos \theta / 4 \tag{5}$$

and the value of microstrain, t = 0.03545 μm and 0.0523 μm

The magnitude of a crystal's crystal defects is shown by the dislocation density, which displays the quantity of dislocation lines per unit



volume of crystal [11]. The following formula is used to determine the dislocation density.

$1/D^2$  which is equal to  $0.02282 \text{ m/m}^3$  and  $0.01046 \text{ m/m}^3$

The values of dislocation density and microstrain have increased in the vanadium-doped cobalt ferrite when compared to the pure form. This shows the presence of vanadium in the material. After comparing the pure and doped forms of vanadium, we may infer from the XRD results above that it is present in the material.

### 3.2 Morphology Investigation

Figure 2 (a -d) shows the FESEM images of the vanadium-doped cobalt ferrite nanoparticles. The images were captured using a Zeiss Gemini Sigma – V. The images were taken at different scales and magnifications. The images were taken in 100 nm and 200 nm. The magnifications at which the images were taken is 100 K and 200 K respectively. As shown in Fig. 2 (a -d), vanadium-doped  $\text{CoFe}_2\text{O}_4$  nanoparticles ( $\sim 20 \text{ nm}$  in diameter) were spherical and tended

to aggregate [21, 22]. The  $\text{CoFe}_2\text{O}_4$  nanoparticles' composition and the near-2:1 atomic ratio of Fe to Co, as well as evidence of vanadium presence, are shown by the EDX analysis of the particles, which is shown in Fig. 1d [23, 24].

### 3.3. Electrochemical Impedance Spectroscopy

The Nyquist pattern for the vanadium-doped cobalt ferrite-coated Ni-foam electrode is displayed in Figure (3). The two main sections of the Nyquist plot are the lower frequency zone, which has a slope, and the higher frequency region, which has a line that resembles a semicircle. Lower resistance is indicated by the semicircle's narrower diameter range. Resistance values of the  $\text{CoFe}_2\text{O}_4$  and Vanadium doped  $\text{CoFe}_2\text{O}_4$  were determined using the Nyquist plot.

The total of the bulk electrolyte, electrode, and contact resistance between the electrode and current collector is the bulk electrolyte resistance, also known as the Equivalent Series Resistance (ESR), which for  $\text{CoFe}_2\text{O}_4$  and Vanadium doped  $\text{CoFe}_2\text{O}_4$  is  $1.22 \Omega$  and  $1.54 \Omega$ , respectively [25].

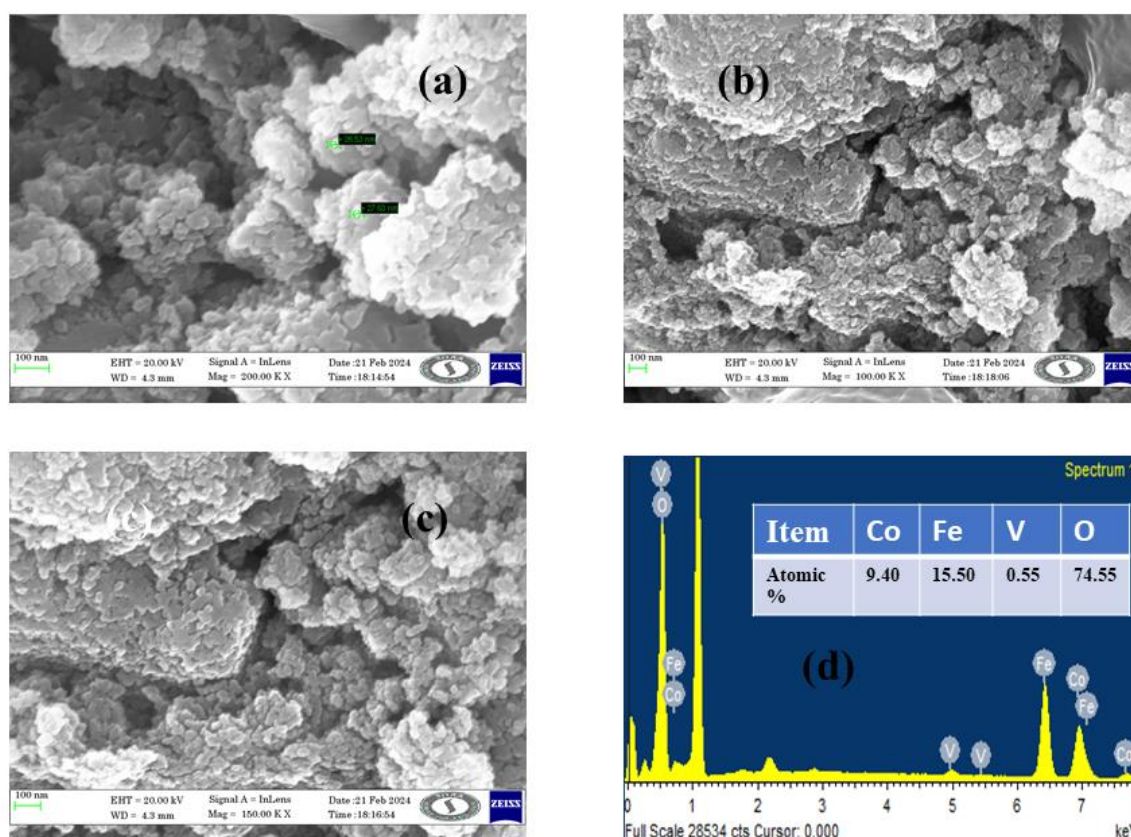


**Figure 2** FESEM images of the vanadium-doped  $\text{CoFe}_2\text{O}_4$  nanoparticles.

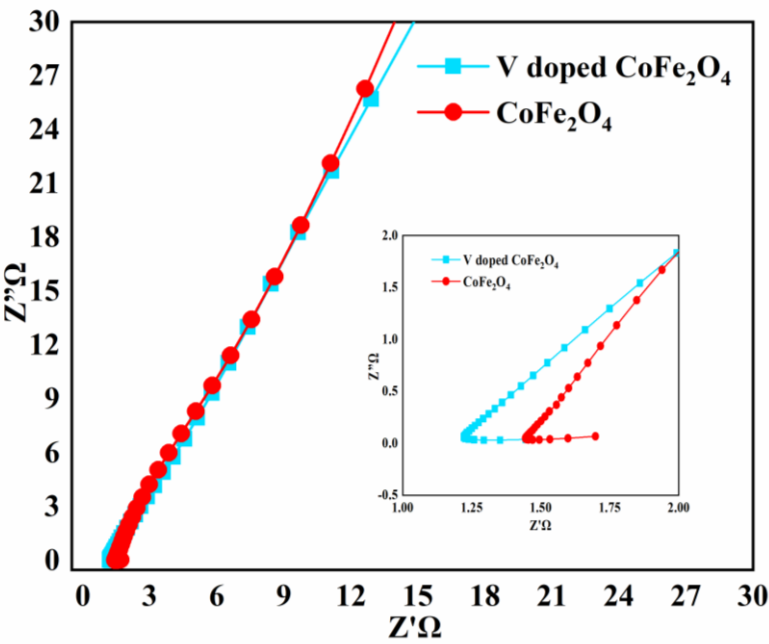


Figure 3 EIS plot of  $\text{CoFe}_2\text{O}_4$  & V doped  $\text{CoFe}_2\text{O}_4$  nanoparticles.

Table 2 EIS Parameters of  $\text{CoFe}_2\text{O}_4$  & V doped  $\text{CoFe}_2\text{O}_4$  nanoparticles

Sample	Equivalent Series Resistance (RA)	Charge Transfer Resistance (RAB)	Internal Resistance (RB)	Warburg Resistance (RBC)
$\text{CoFe}_2\text{O}_4$	1.54 $\Omega$	$1.68 \times 10^{-3} \Omega$	1.5225 $\Omega$	$12.4 \times 10^{-3} \Omega$
V+ $\text{CoFe}_2\text{O}_4$	1.22 $\Omega$	$1.5 \times 10^{-3} \Omega$	1.2215 $\Omega$	$9.3 \times 10^{-3} \Omega$

The Charge Transfer Resistance, also known as the Electrolyte Resistance in the Electrode's pores and the Contact Resistance between the Electrode and Current Collector, is defined as the diameter of the semicircle-like region ( $\text{RAB} = \text{RB} - \text{RA}$ ). The value for  $\text{RAB}$  are  $1.68 \times 10^{-3} \Omega$  and  $1.5 \Omega$  for  $\text{CoFe}_2\text{O}_4$  and Vanadium doped  $\text{CoFe}_2\text{O}_4$  respectively [26].

The charge transfer resistance ( $\text{RB} = \text{RA} + \text{RAB}$ ) and the bulk electrolyte ( $1.2215\text{--}2.225 \Omega$  for  $\text{CoFe}_2\text{O}_4$  and Vanadium doped  $\text{CoFe}_2\text{O}_4$ , respectively) add up to the internal resistance, or  $\text{RB}$  [27].

The line that connects  $\text{RB}$  and  $\text{RC}$  at an intermediate frequency is attributed to either ion transport limitation in the bulk electrolyte or in the electrolyte in porous electrode structures. For  $\text{CoFe}_2\text{O}_4$  and vanadium doped  $\text{CoFe}_2\text{O}_4$ , this line equals  $12.4 \times 10^{-3} \Omega$  and  $9.3 \times 10^{-3} \Omega$ , respectively [19]. This resistance,  $\text{RBC}$ , is called Equivalent Distribution Resistance or Warburg Resistance.

The low resistance values denote that the electrode is a good capacitor. The Parameters of EIS are highlighted in the below table [19, 27].

4. Conclusions

Vanadium-assisted cobalt ferrite nanoparticles made by the co-precipitation process have better structural, morphological, and electrochemical characteristics than pure cobalt ferrite. The synthesized nanoparticles' cubic crystal structure was validated by X-ray diffraction (XRD) analysis, which showed well defined peaks that indicated high crystallinity. Vanadium-doped cobalt ferrite was found to have spherical nanoparticles with an average size of about 20 nm, which indicated a propensity to congregate, according to field emission scanning electron microscopy (FESEM). The elemental composition corresponding with cobalt ferrite and the presence

of vanadium were confirmed by Energy Dispersive X-ray Analysis (EDAX). Vanadium-doped cobalt ferrite's electrochemical performance significantly improved, according to electrochemical impedance spectroscopy (EIS). The equivalent series resistance (ESR) decreased from 1.54  $\Omega$  for pure  $\text{CoFe}_2\text{O}_4$  to 1.22  $\Omega$  for V-doped  $\text{CoFe}_2\text{O}_4$ . The charge transfer resistance decreased from  $1.68 \times 10^{-3} \Omega$  for pure  $\text{CoFe}_2\text{O}_4$  and  $1.5 \times 10^{-3} \Omega$  for V-doped  $\text{CoFe}_2\text{O}_4$ . Additionally, the internal resistance and Warburg resistance values were lower for V-doped  $\text{CoFe}_2\text{O}_4$ , indicating efficient ion transport and storage capabilities. These findings underscore the potential of vanadium-doped cobalt ferrite nanostructures as promising materials for next-generation supercapacitors, addressing critical challenges in energy storage for renewable energy systems.

## References

- [1] G. Behzadi pour, L. Fekri aval, E. Kianfar, Comparative studies of nanosheet-based supercapacitors: A review of advances in electrodes materials. *Case Studies in Chemical and Environmental Engineering* 9 (2024) 100584.  
<https://doi.org/10.1016/j.cscee.2023.100584>
- [2] G.B. Pour, H.N. Fard, L.F. Aval, D. Dubal, Recent advances in Ni-materials/carbon nanocomposites for supercapacitor electrodes. *Materials Advances*, 4, (2023) 6152–6174.  
<https://doi.org/10.1039/D3MA00609C>
- [3] J. Zhang, M. Gu, X. Chen, Supercapacitors for renewable energy applications: A review, *Micro and Nano Engineering* 21, (2023) 100229.  
<https://doi.org/10.1016/j.mne.2023.100229>
- [4] M. Amiri, K. Eskandari, M. Salavati-Niasari, Magnetically retrievable ferrite nanoparticles in the catalysis application. *Advances in Colloid and Interface Science*, 271, (2019) 101982.  
<https://doi.org/10.1016/j.cis.2019.07.003>
- [5] R. Ramadan, M.K. Ahmed, V. Uskoković, Magnetic, microstructural and photoactivated antibacterial features of nanostructured Co–Zn ferrites of different chemical and phase compositions. *Journal of Alloys and Compounds*, 856, (2021).  
<https://doi.org/10.1016/j.jallcom.2020.157013>
- [6] Mmelesi, N. Masunga, A. Kuvarega, T.T. Nkambule, B.B. Mamba, K.K. Kefeni, Cobalt ferrite nanoparticles and nanocomposites: Photocatalytic, antimicrobial activity and toxicity in water treatment. *Materials Science in Semiconductor Processing*, 123, (2021) 105523.  
<https://doi.org/10.1016/j.msssp.2020.105523>
- [7] B. Palanivel, M. Lallimathi, B. Arjunker, M. Shkir, T. Alshahrani, K.S. Al-Namshah, M.S. Hamdy, S. Shanavas, M. Venkatachalam, G. Ramalingam, rGO supported g-C<sub>3</sub>N<sub>4</sub>/CoFe<sub>2</sub>O<sub>4</sub> heterojunction: Visible-light-active photocatalyst for effective utilization of H<sub>2</sub>O<sub>2</sub> to organic pollutant degradation and OH radicals production. *Journal of Environmental Chemical Engineering*, 9(1), (2021) 104698.  
<https://doi.org/10.1016/j.jece.2020.104698>
- [8] H. Sheikhpoor, A. Saljooqi, T. Shamspur, A. Mostafavi, Co-Al Layered double hydroxides decorated with CoFe<sub>2</sub>O<sub>4</sub> nanoparticles and g-C<sub>3</sub>N<sub>4</sub> nanosheets for efficient photocatalytic pesticide degradation. *Environmental Technology & Innovation*, 23, (2021) 101649.  
<https://doi.org/10.1016/j.eti.2021.101649>
- [9] S.B. Bagherzadeh, M. Kazemeini, N.M. Mahmoodi, A study of the DR23 dye photocatalytic degradation utilizing a magnetic hybrid nanocomposite of MIL-53(Fe)/CoFe<sub>2</sub>O<sub>4</sub>: Facile synthesis and kinetic investigations. *Journal of Molecular Liquids*, 301, (2020) 112427.  
<https://doi.org/10.1016/j.molliq.2019.112427>
- [10] S. Farhadi, F. Siadatnasab, A. Khataee, Ultrasound-assisted degradation of organic dyes over magnetic CoFe<sub>2</sub>O<sub>4</sub>@ZnS core-shell nanocomposite. *Ultrason Sonochem* 37, (2017) 298–309.  
<https://doi.org/10.1016/j.ultsonch.2017.01.019>
- [11] T. Baran, M. Nasrollahzadeh, Pd/CoFe<sub>2</sub>O<sub>4</sub>/chitosan: A highly effective and easily recoverable hybrid nanocatalyst for synthesis of benzonitriles and reduction of 2-nitroaniline. *Journal of Physics and Chemistry of Solids*, 149, (2021) 109772.  
<https://doi.org/10.1016/j.jpcs.2020.109772>
- [12] R. Rajangam, N. Pugazhenthiran, S. Krishna, R.V. Mangalaraja, H. Valdés, A. Ravikumar, P. Sathishkumar, Solar light-driven CoFe<sub>2</sub>O<sub>4</sub>/α-Ga<sub>2</sub>O<sub>3</sub> heterojunction nanorods mediated

- activation of peroxymonosulfate for photocatalytic degradation of norflurazon. *Journal of Environmental Chemical Engineering*, 9(5), (2021) 106237. <https://doi.org/10.1016/j.jece.2021.106237>
- [13] F. Hu, W. Luo, C. Liu, H. Dai, X. Xu, Q. Yue, L. Xu, G. Xu, Y. Jian, X. Peng, Fabrication of graphitic carbon nitride functionalized P-CoFe<sub>2</sub>O<sub>4</sub> for the removal of tetracycline under visible light: Optimization, degradation pathways and mechanism evaluation. *Chemosphere* 274, (2021) 129783. <https://doi.org/10.1016/j.chemosphere.2021.129783>
- [14] F. Sharifianjazi, M. Moradi, N. Parvin, A. Nemati, A. Jafari Rad, N. Sheysi, A. Abouchenari, A. Mohammadi, S. Karbasi, Z. Ahmadi, A. Esmailkhanian, M. Irani, A. Pakseresht, S. Sahmani, M. Shahedi Asl, Magnetic CoFe<sub>2</sub>O<sub>4</sub> nanoparticles doped with metal ions: A review. *Ceramics International*, 46(11), (2020) 18391–18412. <https://doi.org/10.1016/j.ceramint.2020.04.202>
- [15] B. Saravanakumar, A. Haritha, G. Ravi, R. Yuvakkumar, Synthesis of X<sub>3</sub>(PO<sub>4</sub>)<sub>2</sub> [X = Ni, Cu, Mn] nanomaterials as an efficient electrode for energy storage applications. *Journal of Nanoscience and Nanotechnology*, 20 (2020) 2813–2822. <https://doi.org/10.1166/jnn.2020.17448>
- [16] M.E.K. Fuziki, R. Brackmann, D.T. Dias, A.M. Tusset, S. Specchia, G.G. Lenzi, Effects of synthesis parameters on the properties and photocatalytic activity of the magnetic catalyst TiO<sub>2</sub>/CoFe<sub>2</sub>O<sub>4</sub> applied to selenium photoreduction. *Journal of Water Process Engineering* 42, (2021) 102163. <https://doi.org/10.1016/j.jwpe.2021.102163>
- [17] S.S. Kolluru, S. Agarwal, S. Sireesha, I. Sreedhar, S.R. Kale, Heavy metal removal from wastewater using nanomaterials-process and engineering aspects. *Process Safety and Environmental Protection*, 150, (2021) 323–355. <https://doi.org/10.1016/j.psep.2021.04.025>
- [18] J.A.Z. Martínez, R.L. Porto, I.E.M. Cortez, T. Brousse, J.A.A. Martínez, L.A.L. Pavón, MnPO<sub>4</sub>·H<sub>2</sub>O as Electrode Material for Electrochemical Capacitors. *Journal of The Electrochemical Society*, 165, (2018) A2349–A2356. <https://doi.org/10.1149/2.1281810jes>
- [19] C.C. Lee, F.S. Omar, A. Numan, N. Duraisamy, K. Ramesh, S. Ramesh, An enhanced performance of hybrid supercapacitor based on polyaniline-manganese phosphate binary composite. *Journal of Solid State Electrochemistry*, 21, (2017) 3205–3213. <https://doi.org/10.1007/s10008-017-3624-1>
- [20] Y. Long, J. Nie, C. Yuan, H. Ma, Y. Chen, Y. Cong, Q. Wang, Y. Zhang, Preparation of CoFe<sub>2</sub>O<sub>4</sub>/MWNTs/sponge electrode to enhance dielectric barrier plasma discharge for degradation of phenylic pollutants and Cr(VI) reduction. *Applied Catalysis B: Environmental*, 283 (2021) 119604. <https://doi.org/10.1016/j.apcatb.2020.119604>
- [21] P. Monisha, P. Priyadharshini, S.S. Gomathi, K. Pushpanathan, Influence of Mn dopant on the crystallite size, optical and magnetic behaviour of CoFe<sub>2</sub>O<sub>4</sub> magnetic nanoparticles. *Journal of Physics and Chemistry of Solids*, 148, (2021) 109654. <https://doi.org/10.1016/j.jpcs.2020.109654>
- [22] C. Li, H. Che, P. Huo, Y. Yan, C. Liu, H. Dong, Confinement of ultrasmall CoFe<sub>2</sub>O<sub>4</sub> nanoparticles in hierarchical ZnIn<sub>2</sub>S<sub>4</sub> microspheres with enhanced interfacial charge separation for photocatalytic H<sub>2</sub> evolution. *Journal of Colloid and Interface Science*, 581, (2021) 764–773. <https://doi.org/10.1016/j.jcis.2020.08.019>
- [23] S. Talukdar, P. Saha, I. Chakraborty, K. Mandal, Surface functionalized CoFe<sub>2</sub>O<sub>4</sub> nanohollowspheres: Novel properties. *Journal of Magnetism and Magnetic Materials*, 513 (2020) 167079. <https://doi.org/10.1016/j.jmmm.2020.167079>
- [24] M. Gao, J. Feng, F. He, W. Zeng, X. Wang, Y. Ren, T. Wei, Carbon microspheres work as an electron bridge for degrading high concentration MB in CoFe<sub>2</sub>O<sub>4</sub>@carbon microsphere/g-C<sub>3</sub>N<sub>4</sub> with a hierarchical sandwich-structure. *Applied Surface Science*, 507, (2020) 145167. <https://doi.org/10.1016/j.apsusc.2019.145167>
- [25] M.M. Emara, S.M. Reda, M.A. El-Naggar, M.A. Mousa, Magnetization and optical bandgap of Cu-Mn vanadate-oxide mixed phase nanostructures. *Journal of Nanoparticle*



- Research, 24, (2022).  
<https://doi.org/10.1007/s11051-022-05607-z>
- [26] A. Song, A.Chemseddine, I.Y. Ahmet, P. Bogdanoff, D. Friedrich, F.F. Abdi, S.P. Berglund, R. van de Krol, Evaluation of Copper Vanadate ( $\beta$ -Cu<sub>2</sub>V<sub>2</sub>O<sub>7</sub>) as a Photoanode Material for Photoelectrochemical Water Oxidation. *Chemistry of Materials*, 32(6), (2020) 2408–2419.  
<https://doi.org/10.1021/acs.chemmater.9b04909>
- [27] N.O. Laschuk, E.B. Easton, O.V. Zenkina, Reducing the resistance for the use of electrochemical impedance spectroscopy analysis in materials chemistry. *RSC Advances*, 11 (2021) 27925–27936.  
<https://doi.org/10.1039/D1RA03785D>

### Does this article screened for similarity?

Yes

### Author contributions

**G. Gowrisankar** - Conceptualization, Methodology, Investigation, Data curation, Writing - Original Draft, Writing—review & editing. **R. Mariappan** – methodology and Data curation, Writing—review & editing. **Emmanuel Feon Ramesh** - Methodology, Data curation and formal analysis. **M. Abishek** - Methodology, Data curation and formal analysis. **M. Prithisha**- Methodology, Data curation and formal analysis, Writing—review & editing. All the authors read and approved the final version of the manuscript.

### Funding

The authors extend their gratitude to the Sri Ramakrishna College of Arts & Science, Coimbatore, India, for their financial support through Research Seed Money Project No. SRCAS/RSM/2022/009.

### Conflict of Interest

The Authors declares that there is no conflict of interest anywhere.

### More Information

This article was part of the Second National Conference on Emerging Materials for a Sustainable Future

(<https://www.psgtech.edu/educms/sorces/CLG/anns/Brochure%20NCEMSF%202024.pdf>), held on July 25–26, 2024, and organized by the Department of Physics, PSG College of Technology, Coimbatore, India.

Title: Proceedings of the Asian Research Association  
 Journal Abbreviation: Proc. Asian Res. Assoc.  
 Publication language: English  
 Publishing Frequency: Continuously updated  
 Month of Publication: July, 2024  
 Subject: Physical Sciences, Chemical Sciences, Engineering, Environmental Science.

### How to cite this article

Gowrisankar, G., Mariappan, R., Ramesh, E. F., Abishek, M., & Prithisha, M. (2024). Electrochemical Impedance Spectroscopy Effects of Vanadium doped-Cobalt Ferrite Nanomaterials for Supercapacitor Applications. *Proceedings of the Asian Research Association*, 1(1), 24-32. doi: 10.54392/ara2413.

### About the License

© The Authors 2024. The text of this article is open access and licensed under a Creative Commons Attribution 4.0 International License.